Paper AAS 02-156

Cassini Orbit Reconstruction From Earth To Jupiter

D. C. Roth, M. D. Guman, R. Ionasescu

Navigation and Mission Design Section, Jet Propulsion Laboratory,
California Institute of Technology, Pasadena, CA 91109

AAS/AIAA Space Flight Mechanics Meeting

San Antonio, Texas 27-30 January, 2002

AAS Publications Office, P.O. Box 28130, San Diego, CA 92129

CASSINI ORBIT RECONSTRUCTION FROM EARTH TO JUPITER

D. C. Roth, M. D. Guman, R. Ionasescu

Navigation and Mission Design Section, Jet Propulsion Laboratory,
California Institute of Technology, Pasadena, CA 91109

This paper describes Cassini reconstructed orbit determination results from the Earth flyby through the Jupiter flyby. Emphasis is placed on orbit determination modeling and the resulting orbit solution. Cassini's encounter with Jupiter occurred on 30 December 2000, with a periapsis time of 10:04:21.870 UTC. Its position relative to Jupiter at closest approach, mapped to the B-plane (see Appendix for B-plane description) in Earth-Mean-Orbital coordinates of J2000, was B•T = 10,896,977 km and B•R = 123,778 km. Formal filtered uncertainties yielded a B-plane error ellipse with a semi-major axis of 115 km, semi-minor axis of 0.6 km, and an orientation angle of 90.7°. The one sigma uncertainty in the time of closest approach was 0.08 seconds.

INTRODUCTION

The purpose of the Cassini mission is to study Saturn and its satellites, rings, and magnetosphere. To accomplish this mission, Cassini's interplanetary trajectory includes gravity assists from two Venus flybys, an Earth flyby, and a Jupiter flyby before injection into orbit around Saturn on 1 July 2004.

Cassini successfully completed its fourth and final planetary gravity assist with closest approach to Jupiter occurring on 30 December 2000. Flying past Jupiter at a periapsis altitude of 9,722,965 km, a ΔV of 2.2 km/s was imparted to Cassini while bending its trajectory by 12.2°. The Earth to Jupiter leg of the Cassini mission was extremely successful as all orbit determination goals and requirements were met. Of the four planned trajectory correction maneuvers between the Earth and Jupiter flybys, only the first two were executed. The last two pre-Jupiter maneuvers were cancelled as the computed spacecraft trajectory was very close to the reference trajectory.

A detailed reconstruction of Cassini's trajectory from Earth flyby to Jupiter flyby is described in this paper. The spacecraft trajectory is characterized first, followed by a description of tracking data and *a priori* models. Reconstructed values are then presented along with tracking data residual plots.

TRAJECTORY DESCRIPTION

The epoch state for the reconstructed trajectory was chosen to be 19 August 1999 02:00 ET, approximately one day after Cassini's closest approach to Earth. Four trajectory correction maneuvers (TCMs) were planned to ensure Cassini's arrival to the targeted aimpoint at Jupiter. TCM13, designed to clean up orbit errors magnified by the Earth flyby, was executed on 31 August 1999. TCM14, designed to satisfy the requirement that a main engine burn of at least five seconds duration be executed every 400 days or less (a "flushing" maneuver), was executed on 14 June 2000. TCM15 and TCM16, the last two Jupiter approach maneuvers, were cancelled because TCM14 placed Cassini on a trajectory very close to the reference trajectory. A fifth TCM was planned after the Jupiter flyby and within the data arc covered by the reconstruction. TCM17, designed to clean up errors magnified by the Jupiter flyby and to satisfy the flushing maneuver requirement, was executed on 28 February 2001.

Salient characteristics of the Cassini trajectory between Earth and Jupiter flybys include the spacecraft geocentric declination, heliocentric range, and Earth-spacecraft-Sun angle (Figure 1). The first 150 days of the trajectory are within five degrees of zero declination, initially limiting the effectiveness of the Doppler tracking data[1]. By mid May 2000, however, the geocentric declination has increased to 20°. Cassini's heliocentric range varied from 1 AU at the Earth flyby to over 5 AU after the Jupiter flyby. This characteristic is significant because it provides an opportunity to distinguish between solar pressure induced accelerations, which vary inversely with the square of the heliocentric range, and radio-isotope thermoelectric generator (RTG) induced accelerations, which are nearly constant. The Earth-spacecraft-Sun plot is of interest because of Cassini's initial Sun-pointed attitude and because of the uncoupled nature of Cassini's Z-thrusters. While maintaining Cassini's attitude, the Z-thrusters impart a ΔV along the spacecraft's –Z axis. Until 1 February 2000, the –Z axis was mostly pointed toward the Sun. Hence, this plot shows how much of the ΔV is immediately visible in the Earth line-of-sight direction. After 1 February 2000, Cassini's –Z axis was mostly pointed at the Earth, so all of the ΔV became visible provided there was tracking coverage.

Noteworthy events included solar opposition on 13 September 1999 and 28 November 2000 and superior solar conjunction on 13 May 2000.

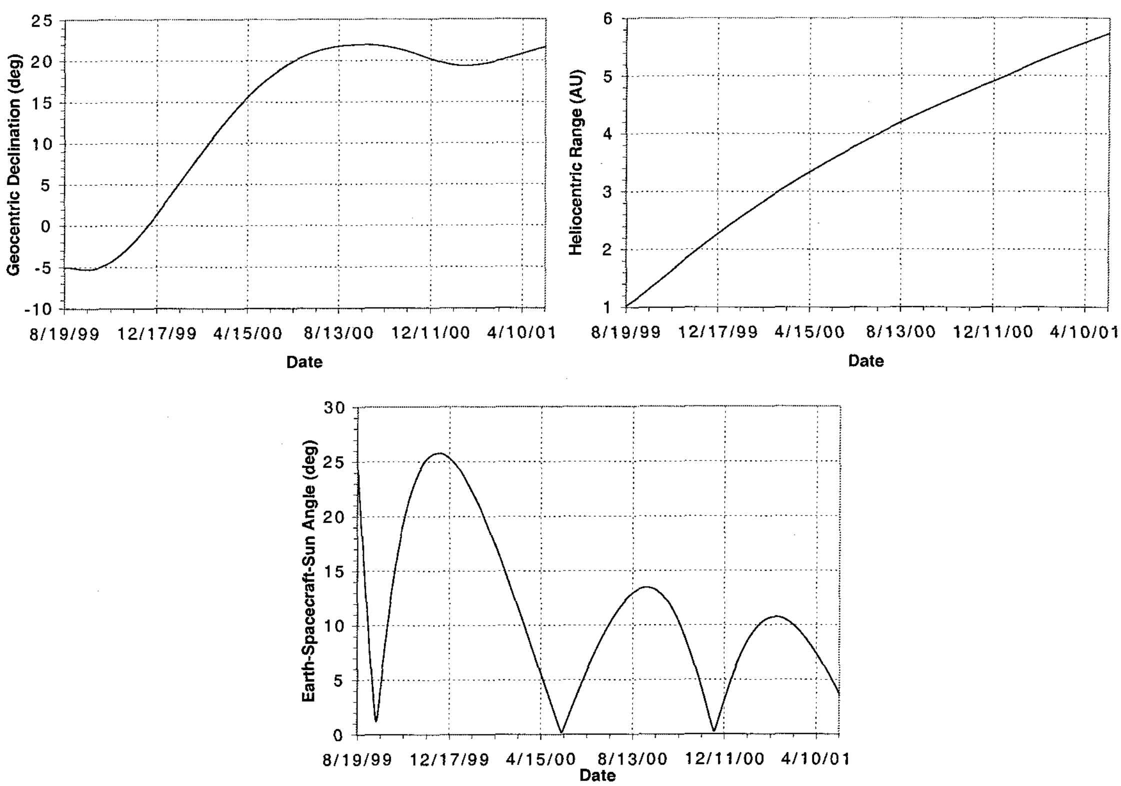

Figure 1 Geocentric Declination, Heliocentric Range, and Earth-spacecraft-Sun Angle

TRACKING DATA

The trajectory reconstruction described in this memo is based primarily on two-way X-band Doppler and range data acquired via Cassini's two low gain antennae (LGA) and high gain antenna (HGA). Except for a four day interval centered on the 13 September 1999 solar opposition, data was collected via Cassini's LGA from the initial trajectory epoch until 1 February 2000. During the four day opposition interval and after 1 February 2000, tracking data was collected via Cassini's HGA. The data arc extends from 19 August 1999 02:02 to 23 March 2001 04:10. Tracking data was deleted between 23 April and 31 May 2000, when the Sun-Earth-Spacecraft angle was within 13° of superior solar conjunction. Troposphere and ionosphere calibrations were applied to all tracking data.

Doppler Data

Two-way Doppler data was compressed to five minute intervals and was weighted at 0.1 mm/s (based on a one minute count time). One half hour of DSS 45/65 three-way Doppler, also compressed to five minute intervals, was fit to allow resolution of two impulsive ΔVs occurring within 1.5 hours of each other. Reaction wheels were spun up at approximately 16:00 UTC on 17 December 2000. At approximately 17:30 UTC, wheels were powered off and allowed to coast to zero RPM. Both activities imparted a ΔV to Cassini and only three-way Doppler was available to resolve them. The three-way Doppler was weighted at 0.2 mm/s (based on a one minute count time).

Range Data

Range data was acquired with integration times varying between five and thirty minutes, and was weighted at 50 m. Range data acquisition via the low gain antenna experienced the anticipated rapid decrease in signal strength as the Earth relative range increased. From the initial epoch until 5 September 1999, range data was accumulated at five minute intervals. From 6 September until 16 October, the interval between range points was increased to 10 minutes to allow adequate correlation of range components. From 17 October until 21 November, a thirty minute interval was required. After 21 November, range data could no longer be successfully acquired via the low gain antenna. Range acquisitions resumed (at five minute intervals) after transitioning to the HGA on 1 February 2000.

A PRIORI MODELS

Radiometric tracking data were combined with *a priori* models to refine estimates of several spacecraft dynamic parameters. In addition, several systematic error sources were 'considered', i.e., some parameter errors were accounted for without actually estimating the parameters themselves. The *a priori* models used for this reconstruction are similar to those discussed in detail in previous publications[2,3]. Where they differ, a detailed description is given. Otherwise, the models are only briefly summarized.

A priori models of estimated parameters include the spacecraft state, non-gravitational accelerations, several ΔV's, and the ephemeris of Jupiter. *A priori* models of considered parameters include the ephemeris of the Earth-Moon barycenter, tracking station locations, and media calibrations.

Spacecraft State and Jupiter Ephemeris

A priori values of the spacecraft state are based on orbit estimates from preceding data arcs. *A priori* uncertainties are essentially infinite, allowing the information content of the tracking data alone to determine the spacecraft state. Jupiter *a priori* ephemeris values and uncertainties are from planetary ephemeris DE405[4].

Non-Gravitational Accelerations

Two accelerations spanning the entire data arc and several others spanning intervals as short as six hours are estimated. Accelerations induced by solar pressure and RTG radiation forces span the entire data arc. Shorter duration accelerations are estimated stochastically to account for variations in attitude control thrusting and mismodeling of the spacecraft attitude.

The acceleration induced directly by solar pressure decreased from 27×10^{-12} km/s^2 just after the Earth flyby to only 0.8×10^{-12} km/s^2 82 days after the Jupiter flyby. These values are based on Cassini Sun pointed attitudes. The acceleration induced *indirectly* by solar pressure, i.e., thruster firings to nullify solar torques, was approximately the same magnitude but acted in nearly the opposite direction - so long as the spacecraft's attitude was controlled with the Reaction Control System (RCS). For much of Cassini's cruise between Earth and Jupiter, however, the spacecraft's attitude was controlled with the Reaction Wheel Assembly (RWA), causing the indirect acceleration to become nonexistent (torques were "unloaded" discretely and modeled as ΔVs). The active attitude control system at any given time can be determined from Table 1.

Direct and indirect solar pressure induced accelerations were modeled via tables of effective areas and effective areas multiplied by effective moment arms respectively. Each tabular value is associated with a specific Sun-relative spacecraft orientation. Accelerations from intermediate spacecraft orientations are interpolated from the table. *A priori* values for the table were determined rather crudely for the most part. An exception is for the spacecraft Sun-pointed effective area, where the HGA shields most of the spacecraft from sunlight. Because the reflectivity coefficients and projected area of the HGA are known fairly well, the *a priori* uncertainty for this value was constrained to 5% of the nominal value. *A priori* uncertainties for the remaining effective areas were fixed at a value representing 20% or greater of the nominal values. *A priori* uncertainties for the indirect accelerations were fixed at a value representing 30% or greater of the nominal values.

Table 1

RCS & RWA ACTIVATION TIMES

Time of Activation	Control Mode	Comment
99 Aug 19	RCS	Trajectory epoch
00 Mar 11	RWA	First test of RWA
00 Mar 27	RCS	
00 Apr 3	RWA	Second test of RWA
00 Apr 21	RCS	
00 May 22	RWA	
00 Jun 13	RCS	TCM14 execution
00 Jun 14	RWA	
00 Sep 19	RCS	CIRS cover release
00 Sep 20	RWA	
00 Dec 16	RCS	RWA anomaly
00 Dec 22	RWA	RWA anomaly recovery
01 Feb 28 1600	RCS	TCM17 execution
01 Feb 28 1845	RWA	

In general, stochastic accelerations were modeled to account for RCS thruster activity that varied from the average solar torque $1/r^2$ model, where 'r' is the spacecraft-Sun distance. Variations from the average model were caused by varying amounts of double-sided limit cycling and coupling between the three controlled axes as deadbands were changed. With the Jupiter science activity beginning 1 October 2000, stochastic accelerations were used to account for spacecraft orientation mismodeling. Numerous science pointing orientation changes were performed and only a limited number of them could be modeled (after 23 February 2001, none were modeled). Stochastic accelerations were estimated to mitigate corruption of solar pressure and RTG radiation acceleration models. A description of stochastic acceleration parameters is included in Table 2.

Table 2

STOCHASTIC NON-GRAVITATIONAL ACCELERATION PARAMETERS

Start Time (ET)	Update Interval	*A Priori* σ (X,Y,Z) x 10^{-12} km/s^2	Control Mode/Comment
99 Aug 19 0200	1 day	(0.5, 0.5, 5)	RCS, 20/20/20 mrad deadbands, LGA active
99 Sep 11 1500	8 hours	(0.5, 0.5, 10)	RCS, 2/2/20 mrad deadbands
99 Sep 15 1200	1 day	(0.5, 0.5, 5)	RCS, 20/20/20 mrad deadbands, LGA active
00 Feb 1 2150	1 day	(0.5, 0.5, 10)	RCS, 2/2/20 mrad deadbands
00 Mar 11 1810	Not estimated		RWA
00 Mar 27 1800	1 day	(0.5, 0.5, 10)	RCS, 2/2/20 mrad deadbands
00 Apr 3 1240	Not estimated		RWA
00 Apr 21 1545	1 day	(0.5, 0.5, 10)	RCS, 2/2/20 mrad deadbands
00 May 22 2130	Not estimated		RWA
00 Jun 13 1750	6 hours	(0.5, 0.5, 10)	RCS, TCM14, 2/2/2 mrad deadbands
00 Jun 14 2000	Not estimated		RWA
00 Sep 19 0835	8 hours	(0.5, 0.5, 10)	RCS, CIRS cover release, 2/2/20 mrad deadbands
00 Sep 20 1440	Not estimated		RWA
00 Oct 1 0800	8 hours	(0.5, 0.5, 0.5)	RWA, Jupiter science pointing mismodeling
00 Dec 16 0100	6 hours	(1000, 1000, 1000)	RCS, RWA anomaly, 2/2/2 mrad deadbands, turns
00 Dec 19 0900	8 hours	(0.5, 0.5, 10)	RCS, anomaly recovery, 2/2/20 mrad deadbands
00 Dec 22 0115	Not estimated		RWA, Jupiter science suspended
00 Dec 29 0200	8 hours	(0.5, 0.5, 0.5)	RWA, Jupiter science pointing mismodeling
01 Feb 23 1800	8 hours	(3,3,3)	RWA, Jupiter science pointing not modeled

In reference 3, the acceleration induced by RTG radiation along the spacecraft Z axis was found to be significantly smaller than the pre-launch estimate. The lesser value was confirmed with the Earth to Jupiter data arc. Therefore, the Z-component *a priori* value was reduced from -7.52×10^{-12} to -3.0×10^{-12} km/s^2 and the *a priori* uncertainty was reduced from 3.76×10^{-12} to 1.5×10^{-12} km/s^2.

ΔV's

Eighty-two ΔV's were estimated including trajectory correction maneuvers 13, 14, and 17. TCM13 and TCM17 were modeled as finite maneuvers, whereas the rest of the ΔV's were modeled as impulsive maneuvers. Many of the ΔV's were imparted by the spacecraft Z-thrusters while the spacecraft was pointed towards the Earth. In these cases, only the spacecraft Z-component coordinate was estimated. *A priori* values were obtained from Doppler data coverage of the ΔV and *a priori* uncertainties were generally set to 0.5 mm/s. For RCS turns, the net ΔV vector was not directed towards the Earth. In these cases, *a priori* values of the spacecraft X- and Y-component coordinates were typically zero, but a large *a priori* uncertainty of several millimeters per second was applied. *A priori* values for TCM13, TCM14, and TCM17 were based on nominal maneuver designs. TCM13 EME2000 RA, Dec, and ΔV nominal values were 76.30°, 24.23°, and 6.696 m/s respectively. TCM17 EME2000 RA, Dec, and ΔV nominal values were 262.86°, -62.09°, and 0.533 m/s. TCM14 EME2000 X, Y, and Z nominal ΔV components were 354.4, 110.3, and 406.4 mm/s. Infinite *a priori* uncertainties were applied to TCM13 and TCM14, allowing an estimate based solely on the tracking data information content. For TCM17, *a priori* uncertainties based on maneuver execution error models were applied.

Considered Parameters

The ephemeris of the Earth-Moon barycenter, tracking stations, and media calibrations were considered. Earth-Moon barycenter ephemeris nominal values and uncertainties are from DE405. Most tracking station location nominal values and uncertainties are from reference 5. DSS 34 (Canberra) and DSS 54 (Madrid) values and uncertainties have been updated to include survey results. Media calibrations are provided by the Tracking System and Analytic Calibration group at JPL. *A priori* uncertainties for dry and wet troposphere calibrations were 1 and 4 cm respectively. *A priori* uncertainties for night and day ionosphere calibrations were 1 and 5 cm respectively.

RECONSTRUCTION VALUES

Estimated values and formal one sigma *a posteriori* uncertainties are listed in Tables 3 – 5. Acceleration and impulsive ΔV estimates are listed in spacecraft fixed coordinates unless stated otherwise. When only one value and uncertainty is listed for a particular impulsive ΔV event, only the spacecraft fixed Z component was estimated. Although direct and indirect solar pressure tabular coefficients were estimated for many different orientations, only estimates for orientations between 165° - 180° co-latitude and at 180° right ascension (direct) and at 180° co-latitude, 180° right ascension (indirect) are listed below. Other estimated tabular coefficients could not be well determined because of spacecraft orientation modeling limitations, limited duration in these attitudes, and the absence of tracking data while in these attitudes.

Table 3

ESTIMATED ACCELERATION VALUES AND UNCERTAINTIES

Acceleration Model		Estimated Value	*a posteriori* sigma
Solar pressure – m^2 (direct)		spacecraft X,Y,Z components	
Colatitude	RA		
165	180	(11.4, -1.0, 20.0)	(3.6, 4.9, 1.6)
170	180	(3.0, -2.6, 18.9)	(3.7, 4.9, 1.3)
175	180	(-14.7, -2.6, 19.6)	(3.4, 5.0, 1.4)
180	180	(-0.9, 0.2, 28.5)	(0.8, 1.1, 1.1)
Solar pressure – m^3 (torque)		Spacecraft X, Y components (Z axis torque controlled with coupled thrusters)	
Colatitude	RA		
180	180	(34.2, -10.6)	(7.9, 6.3)
RTG radiation (km/s^2)		$(-8.1, -1.1, -26.4) \times 10^{-13}$	$(1.1, 0.4, 0.7) \times 10^{-13}$

Table 4

ESTIMATED FINITE BURN VALUES AND UNCERTAINTIES

Event	Time	RA, Dec, ΔV Estimate	*a posteriori* sigma
TCM13 burn only	99 Aug 31 1600	76.340°, 24.51°, 6.683 m/s	(0.005°, 0.04°, 0.002 m/s)
TCM17 & associated turns	01 Feb 28 1730	261.0°, -61.0°, 0.529 m/s	(1.5°, 1.1°, 0.008 m/s)

Table 5

ESTIMATED IMPULSIVE ΔV VALUES AND UNCERTAINTIES

Event	Time	ΔV Estimate (mm/s)	*a posteriori* sigma (mm/s)
Turn HGA to Earth	99 Sep 11 1530	(0, -0.1, -10.2)	(0.5, 0.5, 0.3)
Turn HGA to Sun	99 Sep 15 1200	(0, -0.1, -3.4)	(0.5, 0.5, 0.1)
RWA exercise	99 Sep 17 0645	-1.2	< 0.1
Roll 60.5°	99 Nov 9 1200	-0.7	< 0.1
RWA exercise	99 Dec 6 0215	-1.1	< 0.1
Turn to Masursky & back	00 Jan 23 0340	(-0.6, 0.5, -7.8)	(2.0, 2.0, 1.1)
Turn HGA to Earth	00 Feb 1 2130	(-0.4, -0.2, -9.1)	(2.0, 2.0, 0.8)
Magnetometer calibration	00 Feb 7 0815	(0.5, 7.2, -16.9)	(5.8, 5.9, 0.7)
RWA exercise	00 Mar 4 2157	-1.9	< 0.1
AFC swap	00 Mar 8 0230	-0.7	< 0.1
RWA exercise	00 Mar 9 2135	-2.5	< 0.1
RCS attitude change	00 Mar 10 1825	(2.0, 1.0, -17.9)	(5.3, 4.5, < 0.1)
Transition to RWA	00 Mar 11 1700	-1.0	< 0.1
Momentum unload	00 Mar 15 0623	-1.1	< 0.1
Transition to RCS	00 Mar 27 1800	-4.8	0.5
Transition to RWA	00 Apr 3 1240	-0.1	< 0.1
Momentum unload	00 Apr 13 1503	-2.2	< 0.1
Transition to RCS	00 Apr 21 1545	-3.0	< 0.1
Momentum unload	00 Jun 1 1456	-1.3	< 0.1
Momentum unload	00 Jun 7 1954	-1.2	< 0.1
Transition to RCS	00 Jun 13 1750	-1.4	< 0.1
Main engine cover open	00 Jun 14 0634	-0.4	< 0.1
TCM14 & associated turns*	00 Jun 14 1701	(352.1, 108.1, 393.0)	(0.2, 1.4, 3.3)
Main engine cover close	00 Jun 14 1905	-0.1	< 0.1
Transition to RWA	00 Jun 14 2014	-0.4	< 0.1
Momentum unload	00 Jun 19 1754	-0.9	< 0.1
Momentum unload	00 Jun 22 1555	-0.5	< 0.1
Momentum unload	00 Jun 28 1255	-1.2	< 0.1
Momentum unload	00 Jul 1 1655	-0.9	< 0.1
Momentum unload	00 Jul 7 2155	-1.1	< 0.1
Momentum unload	00 Jul 12 1640	-1.0	< 0.1
Momentum unload	00 Jul 17 1313	-0.7	< 0.1
Momentum unload	00 Jul 22 0800	-0.9	< 0.1
Momentum unload	00 Jul 27 0730	-0.9	< 0.1
Momentum unload	00 Aug 1 1700	-1.1	< 0.1
Momentum unload	00 Aug 7 1837	-1.2	< 0.1
Momentum unload	00 Aug 15 1750	-1.5	< 0.1
Momentum unload	00 Aug 28 1705	-3.1	< 0.1
Momentum unload	00 Sep 7 2025	-1.6	< 0.1
Momentum unload	00 Sep 13 1100	-1.1	< 0.1
Transition to RCS	00 Sep 19 0445	-1.2	< 0.1
CIRS cover release	00 Sep 20 1040	-0.4	< 0.1
Transition to RWA	00 Sep 20 1440	-0.2	< 0.1

Table 5 continued on next page

Table 5 continued from previous page

Event	Time	ΔV Estimate (mm/s)	*a posteriori* sigma (mm/s)
Momentum unload	00 Sep 25 1240	-0.8	< 0.1
RWA friction test	00 Sep 28 0915	-14.3	< 0.1
Momentum unload	00 Oct 4 1205	-0.9	< 0.1
Momentum unload	00 Oct 9 1150	-0.6	< 0.1
Momentum unload	00 Oct 14 1135	-0.5	< 0.1
Momentum unload	00 Oct 19 1110	-0.6	< 0.1
Momentum unload	00 Oct 24 1050	-0.6	< 0.1
Momentum unload	00 Oct 29 1030	-0.7	< 0.1
Momentum unload	00 Nov 3 1010	-0.6	< 0.1
Momentum unload	00 Nov 8 0835	-2.4	< 0.1
Momentum unload	00 Nov 13 0815	-0.7	< 0.1
Momentum unload	00 Nov 18 0710	-0.5	< 0.1
Momentum unload	00 Nov 23 0650	-0.7	< 0.1
Momentum unload	00 Nov 28 0630	-0.7	< 0.1
Momentum unload	00 Dec 3 0610	-0.7	< 0.1
Momentum unload	00 Dec 8 0550	-0.7	< 0.1
Momentum unload	00 Dec 11 0640	-0.5	< 0.1
RWA maintenance	00 Dec 13 1540	-1.9	< 0.1
Momentum unload	00 Dec 15 1135	-0.2	< 0.1
Spin up RWA, anomaly test	00 Dec 17 1600	-2.4	< 0.1
RWA friction test	00 Dec 17 1730	-2.5	0.5
RWA friction test	00 Dec 19 1300	-21.0	0.2
RWA low RPM anomaly test	00 Dec 20 2330	-2.7	0.2
Transition to RWA	00 Dec 22 0115	-2.6	< 0.1
Momentum unload	00 Dec 30 0555	-4.2	< 0.1
Momentum unload	01 Jan 4 0640	-3.1	< 0.1
Momentum unload	01 Jan 9 0750	-2.8	< 0.1
Momentum unload	01 Jan 13 0235	-4.5	< 0.1
Momentum unload	01 Jan 20 0405	-1.4	< 0.1
Momentum unload	01 Jan 29 1815	-0.8	< 0.1
Momentum unload	01 Feb 8 1735	-0.7	< 0.1
Momentum unload	01 Feb 18 1700	-1.9	< 0.1
Transition to RCS	01 Feb 28 1605	-2.4	< 0.1
Transition to RWA	01 Feb 28 1847	-2.8	< 0.1
Momentum unload	01 Mar 10 1545	-2.9	< 0.1
RWA maintenance	01 Mar 15 1800	-1.6	< 0.1
Momentum unload	01 Mar 20 1420	-2.5	< 0.1

* Earth Mean Equator of J2000 coordinates.

Several values listed in Tables 3 – 5 confirm previous estimates. The RTG induced acceleration estimate agrees very closely with the value estimated previously from the Venus 1 to Earth data arc[3]. Estimates of maneuver parameters agree to within one sigma of maneuver reconstructions previously delivered to the Cassini project. *A posteriori* sigmas are significantly smaller than previous values, however (except for TCM17, where the values are nearly the same).

Thirteen additional impulsive ΔV's were modeled but not estimated in the trajectory reconstruction discussed in this paper. These ΔV's are listed in Table 6, where all but two of them are related to TCM13. Because TCM13 was executed while communicating through the LGA, tracking data could be acquired through the wind turns, the TCM, and the unwind turns, allowing them to be estimated separately from the TCM. However, as these ΔV's were grouped closely together, a smaller Doppler compression interval was needed to distinguish them individually. These ΔV's were estimated shortly after execution of TCM13 using a 5 second Doppler compression interval. So that the 5 second Doppler data would not have to be carried along for future analyses, these estimates were fixed and then Doppler data compressed at 5 minute intervals was substituted for the 5 second Doppler data. The last two ΔV's listed in Table 6 occurred near solar conjunction. These values were also estimated previously and then fixed. Because the activities spanned only several minutes and because the ΔV was along the spacecraft to Earth line-of-sight vector, the ΔV's could be estimated reasonably well. Doppler passes within 13° Sun-Earth-spacecraft angle were then deleted so that the biased Doppler passes would not corrupt the orbit data fit.

Table 6

MODELED IMPULSIVE ΔV's WHICH WERE NOT ESTIMATED IN RECONSTRUCTION

Event	Time	ΔV (mm/s)
TCM13 deadband reset	99 Aug 31 1533	(0, 0, -2.8)
Double sided limit cycling	99 Aug 31 1539	(0, 0, -0.2)
TCM13 roll wind turn	99 Aug 31 1543	(0, 0, -0.6)
TCM13 yaw wind turn*	99 Aug 31 1552	(-5.1, 7.4, 4.3)
TCM13 7OFFSET wind turn*	99 Aug 31 1556	(0.8, 3.4, 1.6)
TCM13 7OFFSET unwind turn*	99 Aug 31 1602	(1.2, 3.3, 1.5)
TCM13 yaw unwind turn*	99 Aug 31 1607	(-5.2, 7.4, 4.3)
TCM13 roll unwind turn	99 Aug 31 1616	(0, 0, 0.07)
Double sided limit cycling	99 Aug 31 1618	(0, 0, -0.3)
Double sided limit cycling	99 Aug 31 1655	(0, 0, -0.2)
Double sided limit cycling	99 Sep 1 0150	(0, 0, -0.1)
Transition to RWA (friction transition)	00 May 22 1710	(0, 0, -9.3)
Momentum unload	00 May 26 0332	(0, 0, -0.8)

* Earth Mean Equator of J2000 coordinates.

Stochastic accelerations are displayed in Figures 2 and 3. Sensitivities to attitude control deadbands and Jupiter science pointing activities show that they are serving their intended purpose. The portion of the plot that runs off scale from 16 to 19 December 2000 represents an RWA anomaly. During this period of time several spacecraft turns were executed in RCS mode with 2 mrad deadbands on each axis. These turn ΔV's were modeled solely with stochastic accelerations since tracking coverage was unavailable for a detailed reconstruction of events.

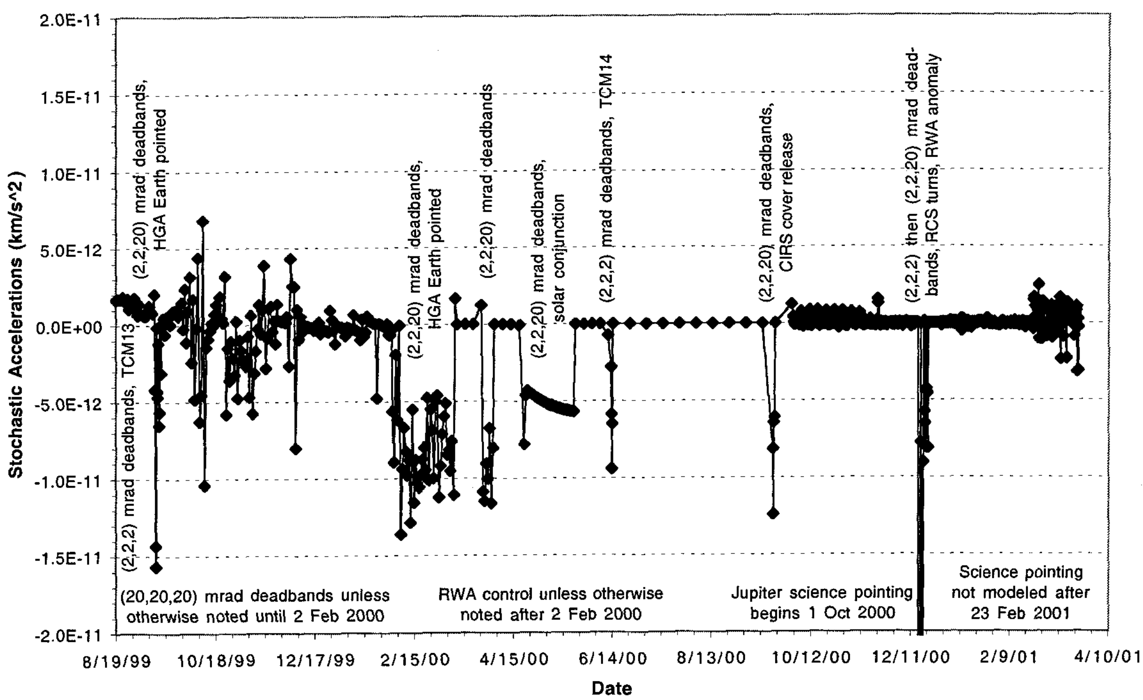

Figure 2 Spacecraft Z-component Stochastic Accelerations

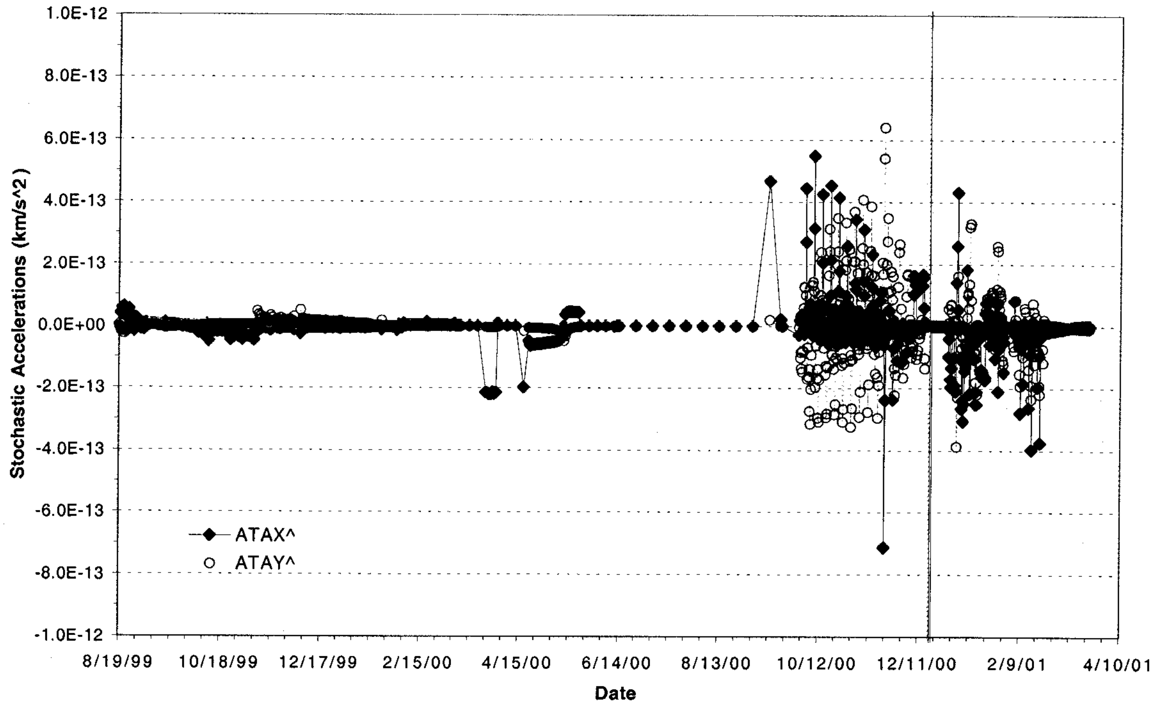

Figure 3 Spacecraft X- and Y-components of Stochastic Accelerations

Jupiter's Sun-centered ephemeris corrections from the DE405 planetary ephemeris at the time of Cassini's closest approach to the planet are 7.9 km radial (R), -66.8 km downtrack (HxR), and –5.3 km out-of-plane (H). Uncertainties on these estimates have improved from the DE405 one sigma values of (12.3, 51.5, 130.7) km to (1.2, 7.4, 96.7) km. Jovian gravitational parameters recommended by Jacobson[6] were used in arriving at these values.

Mapping Cassini's state to the Jupiter B-plane at the time of closest approach yields the values in Table 7. These values are in Jupiter planet-centered, Earth-mean-orbital coordinates of J2000. The corresponding values representing the one sigma error ellipse are 115 km for the semi-major axis, 0.6 km for the semi-minor axis, and 90.7° for the orientation angle.

Table 7

TARGETED & ACHIEVED B-PLANE VALUES AND UNCERTAINTIES

	B•T (km)	B•R (km)	Time of Closest Approach (ET)
Targeted Values	10,896,863	123,618	30 Dec 2000 10:04:43
Achieved Values	10,896,976.8	123,778	30 Dec 2000 10:05:26.053
1σ uncertainties	1.5	115.0	0.079 seconds

Tracking Data residual plots are shown in Figures 4 – 7. Gaps in tracking data from the end of April 2000 through May 2000 correspond to the Sun-Earth-spacecraft angle being less than 13°. A gap in the range data from 20 November 1999 to 1 February 2000 corresponds to the ranging signal strength being too low to enable range data acquisition via the low gain antenna. Other than one half hour of three-way Doppler on 17 December 2000, one-way and three-way Doppler were not included in the reconstruction fit. One-way Doppler drift coefficients were modeled to remove biases from the data and are shown in Table 8.

Table 8

MODELED ONE-WAY DOPPLER DRIFT COEFFICIENTS

Applicable Time Span	Bias Term	Linear Term	Quadratic Term
8/19/99 0200 to 2/1/00 2200	50.202	2.323×10^{-7}	-1.617×10^{-15}
2/1/00 2200 to 10/1/00 0000	53.226	1.873×10^{-7}	-1.051×10^{-15}
10/1/00 0000 to end of arc	56.682	1.488×10^{-7}	-0.837×10^{-15}

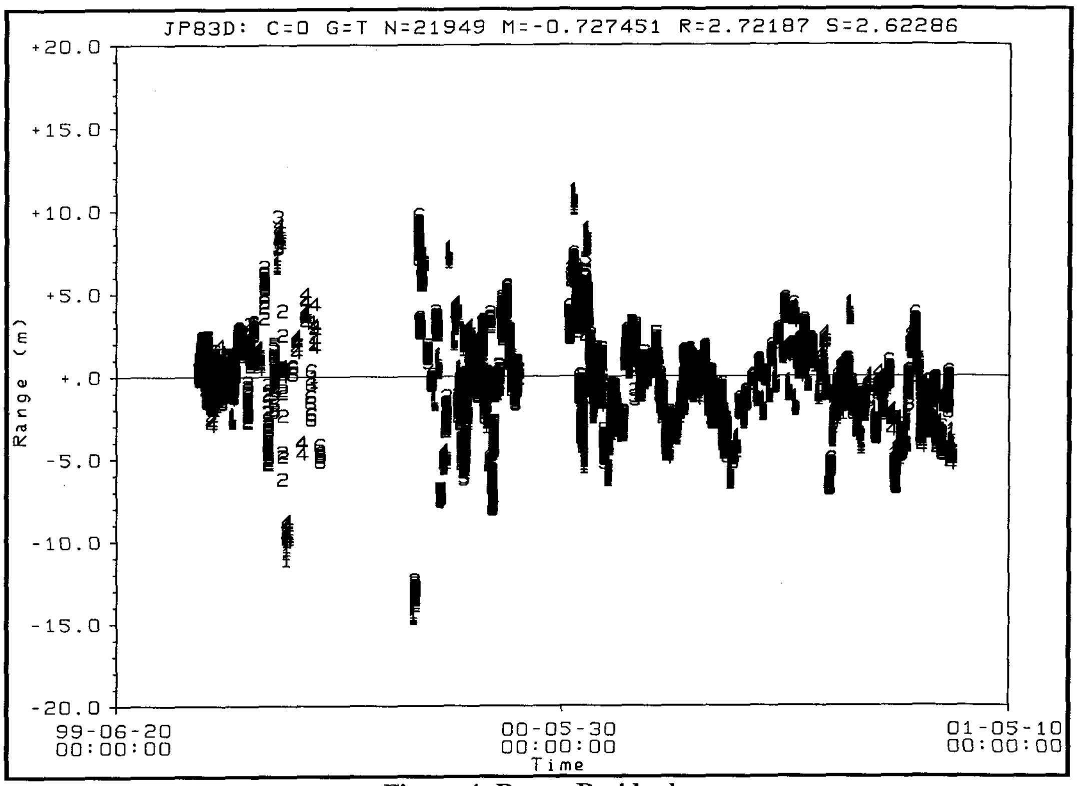

Figure 4 Range Residuals

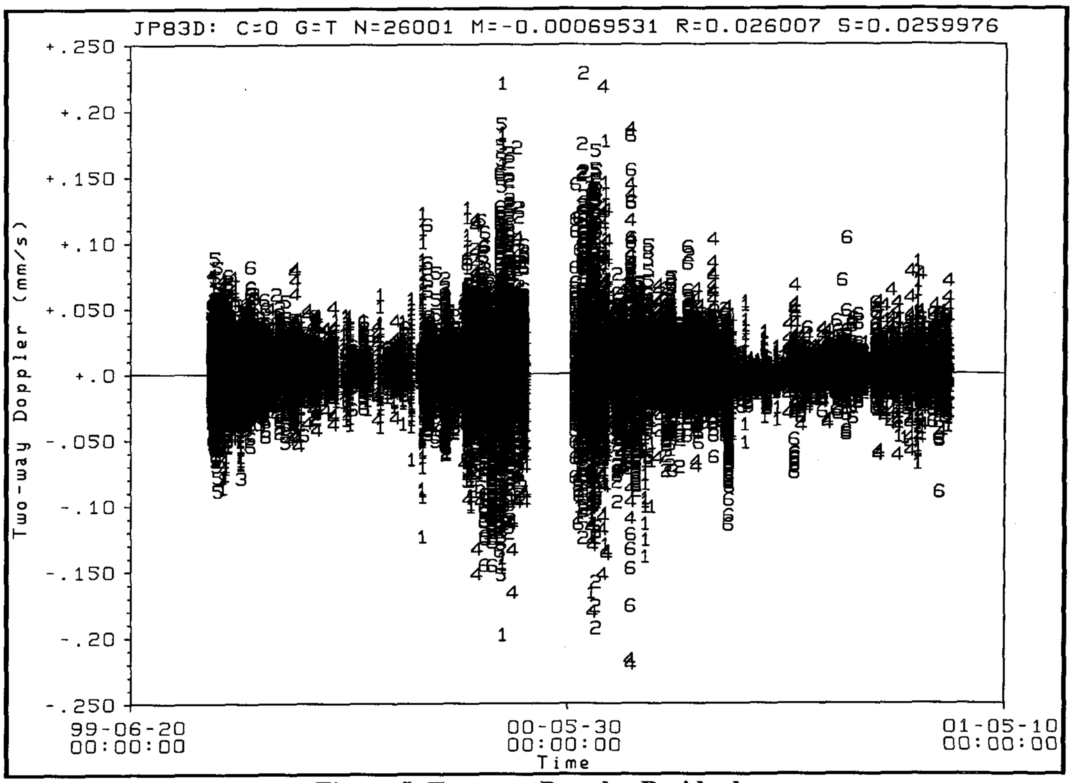

Figure 5 Two-way Doppler Residuals

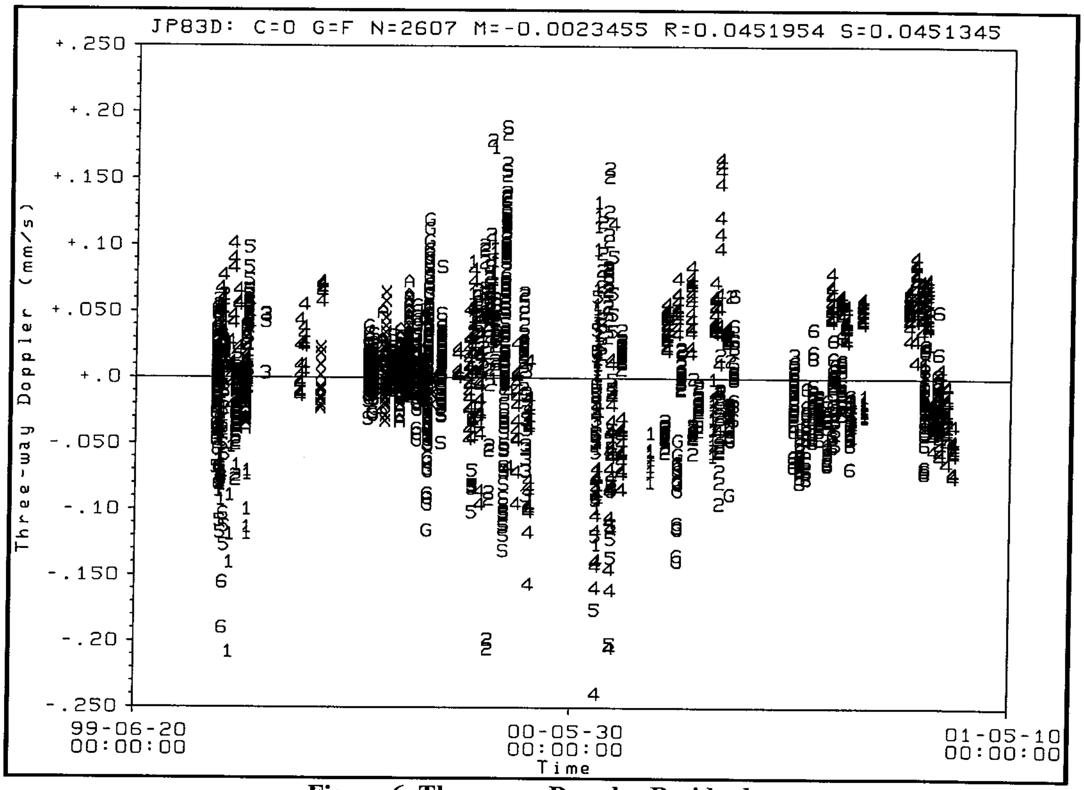

Figure 6 Three-way Doppler Residuals

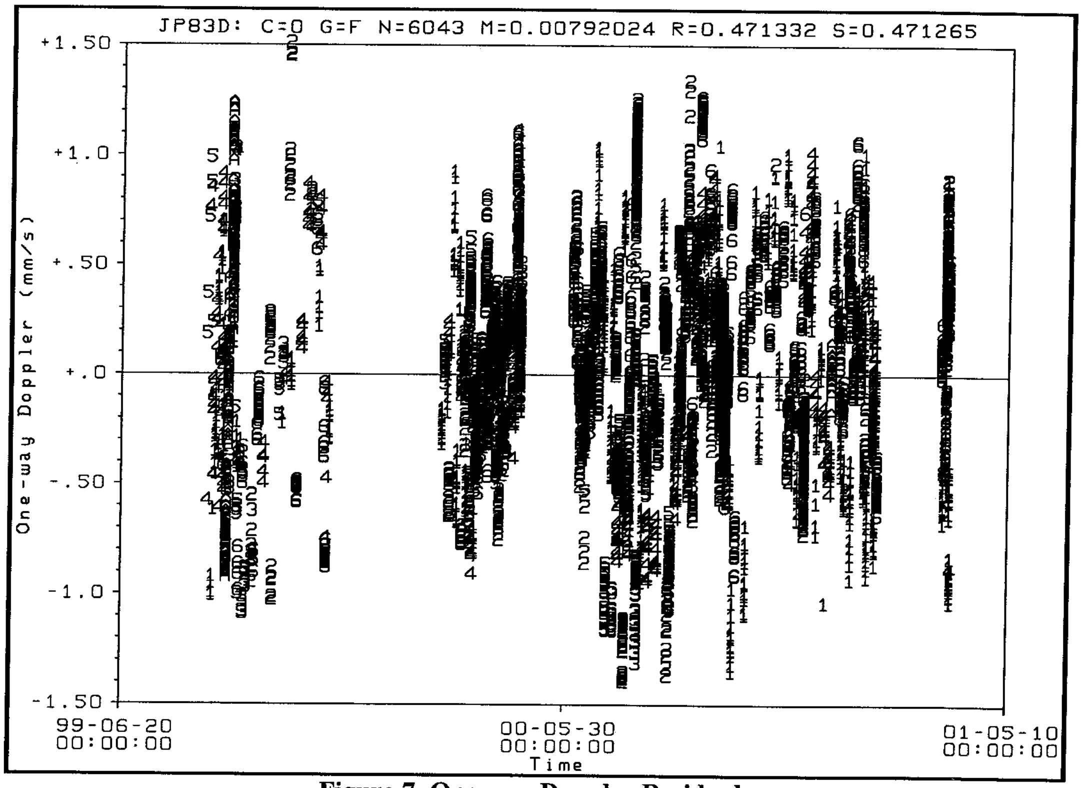

Figure 7 One-way Doppler Residuals

ACKNOWLEDGMENTS

The research described in this paper was performed at the Jet Propulsion Laboratory, California Institute of Technology, under contract with the National Aeronautics and Space Administration.

REFERENCES

1. T.W. Hamilton, W.G. Melbourne, "Information Content of a Single Pass of Doppler Data from a Distant Spacecraft", JPL Space Programs Summary, No. 37-39, Vol. III, March – April 1966, pp. 18-23.
2. D. Roth, M. Guman, R. Ionasescu, A. Taylor, "Cassini Orbit Determination From Launch to the First Venus Flyby", AIAA 98-4563, AIAA/AAS Astrodynamics Specialist Conference, Boston, Massachusetts, 10-12 August 1998.
3. M. Guman, D. Roth, R. Ionasescu, T. Goodson, A. Taylor, J. Jones, "Cassini Orbit Determination From First Venus Flyby to Earth Flyby", AAS 00-168, AAS/AIAA Space Flight Mechanics Meeting, Clearwater, Florida, 23-26 January 2000.
4. E. M. Standish, "JPL Planetary and Lunar Ephemerides, DE405/LE405", ftp://navigator.jpl.nasa.gov/pub/ephem/export/de405.iom, 26 August 1998.
5. W. Folkner, "DSN Station Locations and Uncertainties", JPL TDA Progress Report, 42-128, pp. 1 –34, February 1997.
6. R. A. Jacobson, personal communication, 18 December 2000.

APPENDIX

The B-plane, shown in Figure 8, is a plane passing through the center of the target body and perpendicular to the incoming asymptote of the hyperbolic flyby trajectory. Coordinates in the plane are given in the **R** and **T** directions, with **T** being parallel to the Earth Mean Orbital plane of 2000 (in the direction defined by crossing **S** into the pole vector). The angle θ determines the rotation of the semi-major axis of the error ellipse in the B-plane relative to the T-axis and is measured positive right-handed about S.

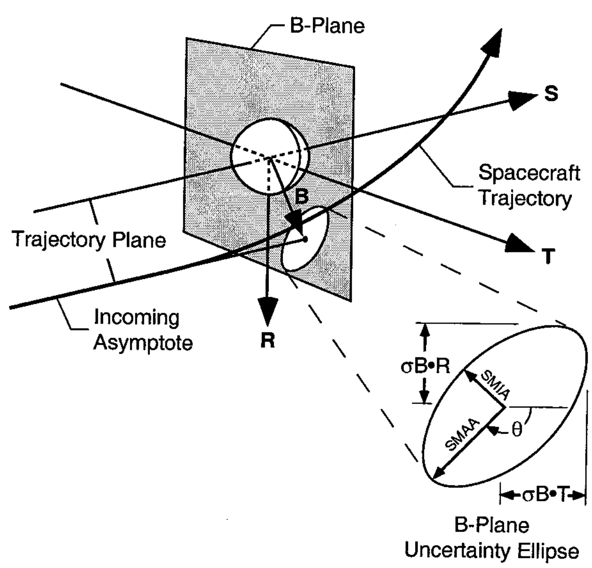

Figure 8 The B-plane Coordinate System